

REVIEW

**OPEN ACCESS**  
Full open access to this and  
thousands of other papers at  
<http://www.la-press.com>.

## Animal Cancer Models of Skeletal Metastasis

Catherine Hibberd<sup>1,2</sup>, Davina A.F. Cossigny<sup>1</sup> and Gerald M.Y. Quan<sup>1,2</sup>

<sup>1</sup>Spinal Biology Research Laboratory, University of Melbourne, Department of Surgery, Austin Health, Heidelberg Victoria 3084, Australia. <sup>2</sup>Department of Spinal Surgery, Austin Health, Heidelberg Victoria 3084, Australia.  
Corresponding author email: [gerald.quan@austin.org.au](mailto:gerald.quan@austin.org.au)

---

**Abstract:** The bony skeleton is one of the most common sites of metastatic spread of cancer and is a significant source of morbidity in cancer patients, causing pain and pathologic fracture, impaired ambulatory ability, and poorer quality of life. Animal cancer models of skeletal metastases are essential for better understanding of the molecular pathways behind metastatic spread and local growth and invasion of bone, to enable analysis of host-tumor cell interactions, identify barriers to the metastatic process, and to provide platforms to develop and test novel therapies prior to clinical application in human patients. Thus, the ideal model should be clinically relevant, reproducible and representative of the human condition. This review summarizes the current *in vivo* animal models used in the study of cancer metastases of the skeleton.

**Keywords:** animal models, skeletal, cancer, metastasis, tumor

---

*Cancer Growth and Metastasis* 2013:6 23–34

doi: [10.4137/CGM.S11284](https://doi.org/10.4137/CGM.S11284)

This article is available from <http://www.la-press.com>.

© the author(s), publisher and licensee Libertas Academica Ltd.

This is an open access article published under the Creative Commons CC-BY-NC 3.0 license.



## Introduction

Primary and secondary cancers are amongst the leading causes of morbidity and mortality. Along with the lung and liver, the bony skeleton is one of the most common sites for metastases, with most cases occurring in the spine.<sup>1-3</sup> Skeletal metastases frequently originate from carcinoma of the breast, prostate, and lung, and if they continue to grow and destroy bone result in pain and pathologic fracture, impaired ambulatory ability and poorer quality of life.<sup>2-7</sup> The process of cancer metastases following tumor growth at the primary site of origin involves intravasation and survival in the bloodstream, arrest, extravasation and finally establishment by invasion and angiogenesis at a distant site.<sup>2,3,8</sup> The ability of metastatic cancer to grow within and invade bone is largely mediated by tumor-induced growth factors and cytokines that result in imbalance between the bone-forming osteoblasts and bone-degrading osteoclasts of bone marrow that normally regulate bone turnover.<sup>2,3,9</sup>

Animal models of cancer metastases are essential in order to better understand the molecular pathways behind metastatic spread and local growth and invasion at distant sites, enable analysis of host and cancer cell interactions, identify barriers to the metastatic process, and to provide potential platforms to develop and test novel therapeutic agents. The ideal model should be clinically relevant, reproducible and representative of the human condition. The broad approaches to animal model studies include spontaneous, chemically or genetically-induced, syngeneic, and xenograft cancer models. Although spontaneous models resemble what occurs when humans develop cancer, the spontaneous development of primary and metastatic cancer in animals is extremely rare.<sup>10</sup> Similarly, the metastasis rate of genetically-induced tumors, either by inducing expression of oncogenes or deletion of tumor suppressor genes, is generally very low and too variable and unpredictable in terms of spreading to bone to provide useful skeletal metastasis models. Therefore, animal models of skeletal metastases typically require physical introduction of cancer cells. Syngeneic models are those in which tumor cells and host are of the same origin and involve introduction of tumor cells isolated from spontaneously occurring rodent or small animal cancers, whereas xenograft models involve the introduction of human tumor cell lines into an immunodeficient host.

Important considerations include the host animal, method of inoculation of tumor cells, type of cancer for investigation, analysis of the developing tumors and clinical application of the model. This paper reviews these considerations, with a specific focus on in vivo animal models of cancer metastases to the bony skeleton.

## Host Animal for Cancer Metastasis Models

Considerations for the choice of host animal to be used for studying cancer and metastasis include animal availability, cost, handling, desired cancer type for investigation, technique of introduction of cancer cells, and whether surgical procedures are required for tumor implantation or treatment, as well as how the resulting tumors and tissues are to be imaged and analyzed. Established animal models used for studying skeletal metastases are summarized in Table 1.

To date, the rodent has been the most popular host animal used in the study of bone metastases.<sup>8</sup> Rodents have a high degree of gene sequence homology with humans, similar anatomical organs, are easy to handle and maintain, readily available and relatively cheap, and can be manipulated for investigation of specific cancer pathways by generating knockout, transgenic, or over-expressing strains.<sup>11,12</sup> Immune-deficient animals such as *Balb/c* athymic nude mice and severe combined immunodeficiency (SCID) mice are commonly used in xenograft models as they are unable to immunologically reject transplanted tissue or cells, thus enabling the study of human cancer cell lines. As SCID mice are more severely immunocompromised than nude mice, it has been suggested that some cancer cell lines may grow more rapidly or produce a higher incidence of metastases in SCID compared with nude mice.<sup>13</sup> Strube et al described a mouse model of human renal cell carcinoma metastasizing to bone following intracardiac inoculation of human 786-O/luciferase cells into nude mice, resulting in aggressive osteolytic bone lesions involving the hindlimbs, forelimbs, pelvis, and spine.<sup>14</sup> Similarly, Garcia et al injected a bone metastasizing-only subclone (B02) from the MDA-MB-231 human breast cancer cell line into the tail vein of nude mice, resulting in osteolytic bone metastases of the hindlimb.<sup>5</sup>

One of the disadvantages of using immunodeficient animals in models of cancer metastases is that

**Table 1.** Established *in vivo* animal models of skeletal metastases.

| Ref. | Animal                         | Cancer cell line  | Method of inoculation                           | Location of skeletal metastases     | % Success rate for skeletal metastases       | Observed metastases in other organs  |
|------|--------------------------------|---|---|-------------------------------------|--|--------------------------------------|
| 21   | <b>MOUSE</b><br>Female C57BL/6 | <b>MURINE MELANOMA</b><br>B16-G3.26                                   | Intracardiac                                    | Spine, long bones, pelvis           | >95%   | Lungs, liver, ovaries                |
| 33   | C57BL/6                        | B16-F10   | Intracardiac                                    | Spine, long bones, pelvis           | 100%   | Visceral                             |
| 1    | Female C57BL/6                 | B16-G3.26   | Intracardiac                                    | Spine                               | NS   | NS                                   |
| 6    | Female C57BL/6                 | B16-F1  | Intracardiac                                    | Femur                               | 60–100%                                      | Visceral                             |
| 37   | C57BL/6<br>(immunocompetent)   | <b>MURINE PROSTATE CA</b><br>RM1<br>(bone metastasizing subclone)     | Intracardiac                                    | Spine, long bones, skull, scapula   | >95%   | Kidney, adrenals, other soft tissues |
| 32   | Male SCID                      | <b>HUMAN PROSTATE CA</b><br>PC-3                                      | Orthotopic                                      | n/a                                 | n/a  | n/a                                  |
| 10   | Nude                           | PC-3<br>(PC-3M highly metastatic sub-line)                            | Intracardiac                                    | Spine, long bones                   | NS   | NS                                   |
| 9    | Male nude                      | IGR-CaP1  | Intracardiac<br>Orthotopic (tibia)              | Spine, long bones, mandible         | 55%<br>(intracardiac)                        | Liver, lung, kidney                  |
| 22   | Female nude                    | <b>HUMAN BREAST CA</b><br>MDA-MB-231<br>(bone-metastasizing subclone) | Intracardiac<br>Tail vein<br>Orthotopic (tibia) | Spine, long bones                   | 100%<br>(intracardiac)<br>Nil from tail vein | Brain, lung<br>(intracardiac)        |
| 31   | Female nude                    | MDA-MB-231  | Orthotopic (tibia)                              | n/a                                 | n/a  | n/a                                  |
| 25   | Female nude                    | MDA-MB-231  | Intracardiac                                    | Femur                               | NS   | Lung                                 |
| 5    | Female nude                    | MDA-MB-435  | Mammary fat pad                                 |                                     |  |                                      |
| 4,29 | Female nude                    | MDA-MB-231<br>(B02 subclone)  | Tail vein                                       | Long bones                          | NS   | Nil                                  |
| 41   | Female nude                    | MDA-MB-231<br>(F10 subclone)  | Orthotopic (femur)                              | n/a                                 | n/a  | n/a                                  |
| 41   | Female nude                    | MDA-MB-435  | Intracardiac                                    | Spine, long bones, pelvis, mandible | NS   | NS                                   |
| 15   | Female nude                    | <b>MURINE BREAST CA</b><br>4T1.2                                      | Intracardiac                                    | Spine, femur                        | 65% (4T1.2)                                  | Lung                                 |
| 35   | Female nude                    | 4T1<br>67NR<br>66c14  | Tail vein<br>Mammary fat pad                    |                                     |  |                                      |
| 1    | Female nude                    | 4T1E/M3   | Tail vein                                       | Spine                               | 70% (4T1E/M3)                                | Lung                                 |
| 14   | Female nude                    | 4T1E  | Subcutaneous                                    | Spine                               | 100%   | NS                                   |
| 14   | Female nude                    | 786–0<br>(highly metastatic subclone)                                 | Intracardiac                                    | Spine, long bones                   | 100%   | Nil                                  |
| 42   | SCID                           | ACHN  | Orthotopic (lamina)                             | n/a                                 | n/a  | n/a                                  |

(Continued)

**Table 1.** (Continued)

| Ref.  | Animal              | Cancer cell line  | Method of inoculation                    | Location of skeletal metastases | % Success rate for skeletal metastases | Observed metastases in other organs |
|-------|---------------------|---|--|---------------------------------|--|-------------------------------------|
|       | <b>MOUSE</b>        | <b>HUMAN RCC</b>  |  |                                 |  |                                     |
| 12    | Nude                | <b>HUMAN LUNG CA</b><br>PC-14                           | Orthotopic<br>(L3 vertebra)              | n/a                             | n/a                                    | n/a                                 |
| 32    | Male SCID           | H460  | Orthotopic                               | n/a                             | n/a                                    | n/a                                 |
|       |                     | <b>MOUSE LYMPHOMA</b>                                   |  |                                 |  |                                     |
| 23    | Female nude         | A20   | Tail vein                                | Spine                           | 80%                                    | Liver, lymph nodes                  |
|       |                     | <b>HUMAN FOLLICULAR THYROID CA</b>                      |  |                                 |  |                                     |
| 43    | Male nude           | WRO   | Orthotopic (tibia)                       | n/a                             | 80%                                    | n/a                                 |
|       |                     | <b>HUMAN NEUROEPITHELIOMA</b>                           |  |                                 |  |                                     |
| 1     | Nude                | SK-N-MC   | Intracardiac                             | Spine                           | NS                                     | NS                                  |
|       |                     | <b>HUMAN CERVICAL ADENOCA</b>                           |  |                                 |  |                                     |
| 1     | Nude                | HeLA  | Intracardiac                             | Spine                           | NS                                     | Intradural, brain                   |
|       |                     | <b>RAT</b>  |  |                                 |  |                                     |
| 27    | Female nude         | <b>HUMAN BREAST CA</b><br>MDA-MB-231<br>(RBC3 subclone) | Intracardiac                             | Spine, long bones               | 50–86%                                 | NS                                  |
| 28    | Female nude         | MDA-MB-231  | Orthotopic<br>(L5 vertebra)              | n/a                             | n/a                                    | n/a                                 |
| 30    | Nude                | MDA-MB-231  | Intra-arterial                           | Hindlimb long bones             | 100%                                   | Nil                                 |
| 38    | Female nude         | MT-1  | Intracardiac                             | Spine                           | 100%                                   | NS                                  |
| 39    | Nude                | MT-1  | Intracardiac                             | Spine                           | NS                                     | NS                                  |
| 40    | Nude                | MT-1  | Intracardiac                             | Spine                           | 80%                                    | Intradural                          |
|       |                     | <b>RAT MAMMARY CA</b>                                   |  |                                 |  |                                     |
| 36,44 | Female nude         | CRL-1666  | Orthotopic<br>(L6 vertebra)              | n/a                             | n/a                                    | n/a                                 |
| 24    | Male wistar         | Walker 256  | Intra-arterial                           | Hindlimb long bones             | 90%                                    | Nil                                 |
|       |                     | <b>RABBIT</b>   |  |                                 |  |                                     |
| 17,26 | New Zealand white   | <b>RABBIT CARCINOMA</b><br>VX2                          | Orthotopic<br>(thoracic vertebra, tibia) | n/a                             | n/a                                    | n/a                                 |
| 16    | Male Japanese white | VX2   | Orthotopic (L3 vertebra)                 | n/a                             | n/a                                    | n/a                                 |
|       |                     | <b>DOG</b>  |  |                                 |  |                                     |
| 20    | Mongrel dogs        | <b>DOG PROSTATE CA</b><br>DPC-1                         | Prostate                                 | Pelvis                          | 15%                                    | Lung, lymph nodes                   |

**Abbreviations:** NS, not specified; n/a, not applicable (given direct inoculation of tumour cells into bone); SCEA, superficial caudal epigastric artery (to hindlimb); CA, carcinoma; RCC, renal cell carcinoma.



they preclude investigation into the important role of the immune system in combating cancer.<sup>11</sup> This may be overcome by the use of syngeneic models, in which cancer cell lines of the same species as the host are introduced into immunocompetent animals. Lelelakis et al described a mouse model of breast cancer metastases to bone using a clonal tumor cell line from a spontaneously arising murine mammary cancer, in which metastases to the femur and spine followed intracardiac and mammary pad inoculation of the cancer cells.<sup>15</sup> Another disadvantage of rodent cancer models includes the small size of rodent bone, potentially making direct implantation of cancer cells, as well as investigation of therapeutic modalities such as local drug delivery devices and invasive image-guided-therapies, more technically challenging.<sup>12,16,17</sup>

The use of rabbits may be less technically demanding for surgical procedures and may enable easier analysis and preclinical testing of skeletal metastases. However, experimental immunodeficient rabbits are currently not available; thus, species-specific cancer cell lines are required in rabbit syngeneic cancer models and these are extremely limited in availability.<sup>11,16,17</sup> Despite this, VX2 carcinoma cells derived from a virus induced papilloma of the rabbit have been used in two rabbit models of spinal tumors to successfully replicate the clinical, radiological, and histopathologic characteristics of the human condition.<sup>16,17</sup> Orthotopic implantation of the VX2 carcinoma cells into the third lumbar vertebra or the lower thoracic vertebra of healthy rabbits after surgical exposure led to lower limb paralysis in most rabbits by four weeks post-implantation.

Larger-sized animals that can potentially be used in cancer models include the cat and dog. Although the cat has not yet been established as a useful syngeneic or xenograft animal model for the study of skeletal metastasis, spontaneous metastases to the digits of the bony skeleton and in soft tissues of the proximal limbs in cats have been observed secondary to primary pulmonary adenocarcinoma.<sup>18,19</sup> In a larger syngeneic orthotopic animal model, a dog model of prostate cancer metastasis, Anidjar et al demonstrated bone metastases following direct inoculation of DPC-1 poorly differentiated canine prostate adenocarcinoma cells into the prostate gland.<sup>20</sup> Histopathology of the mixed osteoblastic and osteolytic pelvic bone lesions showed similarities to human prostate

cancer skeletal metastases.<sup>20</sup> A potential advantage of the larger canine model over rabbits or rodents is that dogs may be more amenable to diagnostic and surgical procedures with equipment used in human clinical practice; however, the cost and restricted availability of the animals and species-specific cancer cell lines remain limitations.

## Inoculation of Cancer Cells

As described above, since the spontaneous development of metastatic cancer in animals is rare and unpredictable, animal models of skeletal metastases typically require physical introduction of cancer cells. Commonly used methods of cancer cell inoculation include systemic intracardiac or tail vein injection, injection into the arterial circulation, direct inoculation into the primary cancer site such as the mammary fat pad or prostate gland, or direct orthotopic inoculation into bone, reproducing the secondary skeletal deposit in isolation (Table 1).

Models involving systemic dissemination of tumor cells permit investigation of the key elements of the metastatic cascade from survival within the bloodstream, to selection of a distal site, and eventually to extravasation, establishment and growth of distant metastases, thus allowing analysis of the molecular mechanisms involved in growth and proliferation, migration, invasion and angiogenesis of metastatic cancer cells.<sup>11,15</sup> Intracardiac injection into the left ventricle results in systemic arterial circulatory dissemination of tumor cells, with the potential of generating widespread metastases. Arguello et al described a reproducible murine model of skeletal vertebral and long bone metastasis following intracardiac injection of B16 (sub-line G3.26) murine melanoma cells.<sup>21</sup> However, the sites of metastatic deposition and number and size of the metastases were unpredictable, extremely variable, and dependent on the amount of cancer cells administered. The quantity of resultant bone metastases increased with increasing number of cells injected.

Tail vein inoculation similarly results in hematogenous dissemination of cancer cells, although cells may be filtered and cleared by the pulmonary system during the first passage through circulation.<sup>22</sup> Passineau et al described tail vein injection of A20 murine lymphoma cells to generate a syngeneic mouse model to mimic disseminated human B cell lymphoma,



with bony deposits to the femur, pelvis and vertebral column, eventually leading to bone destruction and nerve compression.<sup>23</sup> Biesalski et al described intra-arterial injection of Walker 256 mammary carcinoma cells directly into the circulation of the hindlimbs in rats via the superficial caudal epigastric artery, a branch of the femoral artery, resulting in metastases to the distal femur or proximal tibia/fibula in 9 of 11 animals at 3 weeks post-inoculation.<sup>24</sup> Limitations of systemic administration of tumor cells include variability and unpredictability in site, size, number, and time to development of metastasis.<sup>10,11</sup> This may also lead to excessive tumor burden and morbidity in the experimental animal, therefore precluding the ability to investigate potential therapeutic interventions.

Direct inoculation of tumor cells into primary sites such as the mammary fat pad also has the potential to create a complete model of the metastatic process, since the tumor must first establish in the primary site before seeding to distant sites.<sup>15</sup> Schubert et al described a mouse model of breast cancer metastasis to the femur and lung after MDA-MB-435 human breast cancer cells were injected into the mammary fat pad of nude mice.<sup>25</sup> The ability of gonadotropin-releasing hormone (GnRH) analogs to significantly reduce formation and growth of breast cancer metastases in this model suggested the multi-focal role of GnRH throughout the metastatic process of breast cancer, including epithelial-mesenchymal transition, migration, invasion, and biology of circulating cells.

Direct orthotopic inoculation into bone has the potential to produce reproducible, efficient, and site-specific models of cancer and metastasis since a known quantity of cancer cells can be directly administered into the target bone of choice. Direct inoculation into bone bypasses the metastatic cascade and is not a true model of metastases, nevertheless it permits targeted investigation of the cellular processes involved within a particular anatomical site and the local effects of the tumor itself. Mann et al described a mouse model of tumor-induced osteolysis following orthotopic injection of F10 human breast cancer cells into the distal femoral metaphysis to assess the ability of non-invasive imaging and computational techniques for predicting the strength of bones with osteolytic lesions.<sup>4</sup> Choi et al used direct orthotopic inoculation of VX2 carcinoma tissue fragments into the tibial shaft of rabbits to create a model for

magnetic resonance imaging (MRI) and histopathologic evaluation of the evolution of metastatic bone tumor.<sup>26</sup> Orthotopic inoculation may be a relatively straightforward procedure if prominent and subcutaneous bones are selected, such as the distal femur or proximal tibia, which are also common sites for primary and secondary bone cancers. In our own laboratory, we recently established a novel in vivo model of spinal cancer that causes a reproducible, evolving paraplegia following orthotopic inoculation of MDA-231 human breast cancer cells or PC-3 human prostate cancer cells into the vertebral body at the thoracolumbar junction of *Balb-c* athymic nude mice (Fig. 1). The progressive neurological decline in the animals, from gait asymmetry and unilateral hindlimb weakness, to complete unilateral hindlimb paralysis and finally to complete bilateral hindlimb paralysis, closely resembles the natural history of untreated metastatic epidural spinal cord compression and potentially enables closer analysis of the temporospatial pattern of cancer growth within the spine and the molecular mechanisms behind this devastating condition.

## Cancer Cell Lines

Amongst the commonest primary cancers that metastasize to bone are breast, prostate, lung, and renal, carcinoma. Since the biological behavior and response to therapy of bone metastases is largely dependent on the primary cancer type, there is a need to develop investigative models of varying cell lines. For example, prostate cancer bone metastases in humans are generally more osteoblastic or sclerotic in nature, while renal cell carcinoma bone metastases are often more lytic and vascular compared with other cancer types.<sup>2,3,14</sup> Indeed, a sub-line of the 786-O human renal cell carcinoma cell line with increased bone metastatic potential showed higher expression of the pro-angiogenic factors VEGF and basic fibroblast growth factor (bFGF) compared with the parental cell line.<sup>14</sup>

Immortalized cancer cell lines that are generated through isolation of tumor cells from these spontaneously occurring primary or secondary cancer types in humans or animals are ideal for use in in vivo cancer models as they have already demonstrated ability to form, grow, invade, and spread within the primary organ or metastatic site of choice. Human cancer cell lines with a propensity for localization to

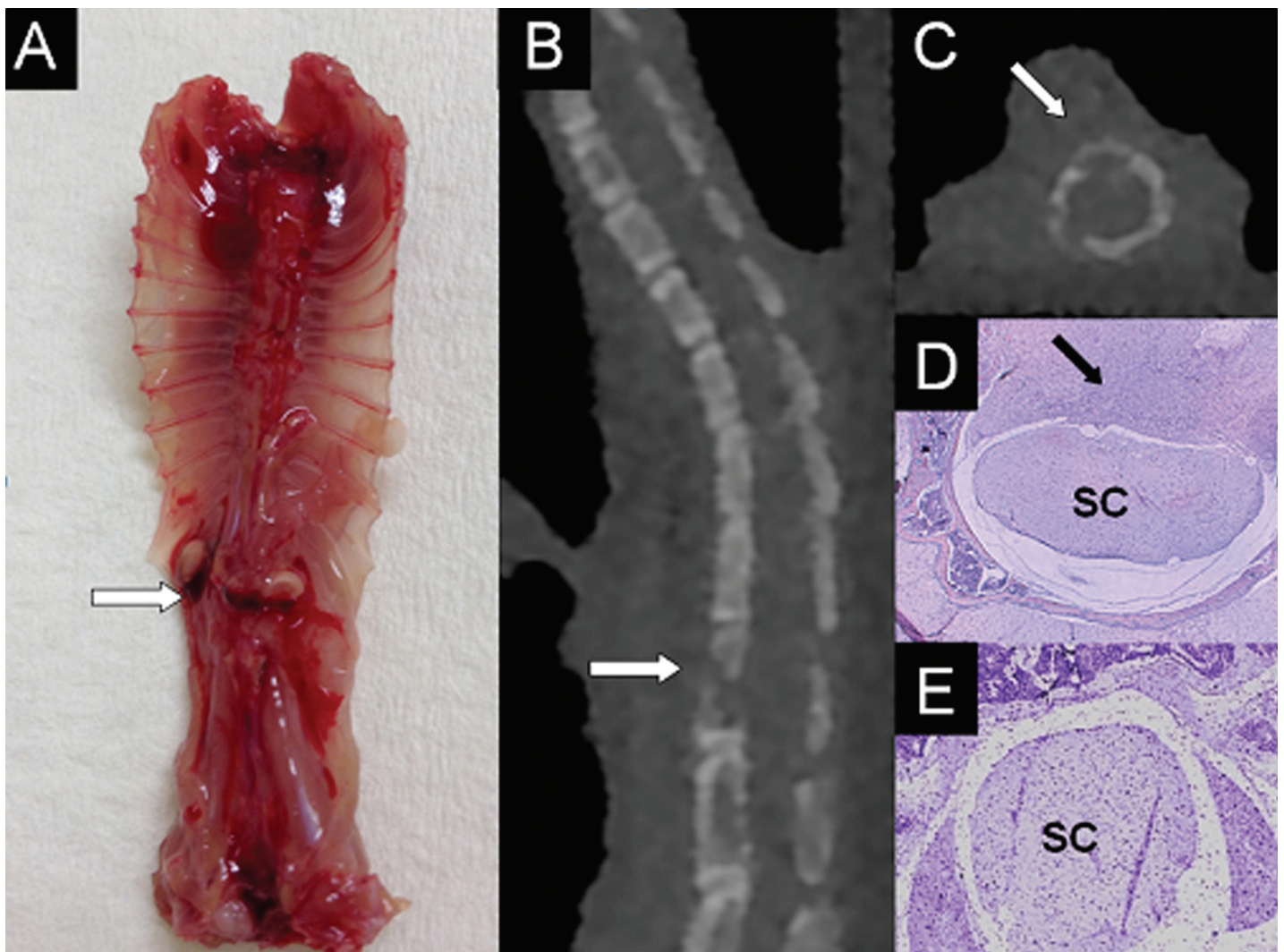


**Figure 1.** Representative images of established spinal cancer (arrows) following orthotopic injection of PC-3 human prostate cancer cells in the vertebral body of the thoracolumbar junction in a nude mouse. **A)** Dissected spine specimen; **B)** Sagittal, and **C)** axial micro-CT images demonstrating lytic bony lesion and cortical destruction; **D)** Histological cross-section showing tumor invasion of vertebral bone marrow and encroachment onto the spinal cord (SC); **E)** Control histological cross-section.

bone and that are well-established for use in animal cancer metastasis models of metastases include the MDA-MB-231 human breast cancer cell line isolated from the pleural effusion of a patient following breast cancer metastasis to the lungs,<sup>5,22,27-31</sup> and PC-3 human prostate cancer cells derived from a bone metastasis.<sup>8,9,32</sup> The use of cancer cell lines of human origin ensures that molecular and histologic analysis is as comparable to the human condition as possible; however, one important limitation is the requirement for use of an immunocompromised animal, which precludes investigation of the host immune response to the development of cancer and metastases.<sup>11</sup> The B16 murine melanoma cell line, derived from a melanoma from the skin of a C57BL/6 strain mouse,<sup>6,21,33</sup> and

the VX2 rabbit carcinoma cell line, originated from a carcinoma induced by the Shope cottontail rabbit papilloma virus,<sup>16,17,26</sup> are common animal cell lines used in models of skeletal metastasis models that exhibit similar molecular characteristics to human cancer cells.

Cell sub-lines with site-specific metastatic properties, such as the propensity to metastasize to the skeleton, are often generated from primary cell lines through serial culture and repeated injection of cells cultured from metastatic lesions at the site of interest. For example, Zadnik et al derived a novel cell sub-line, RBC-3, from human MDA-MB-231 breast cancer metastatic spinal lesions in a rat.<sup>27</sup> Parent MDA-MB-231 human breast adenocarcinoma cells



were introduced by intracardiac injection into rats to induce metastatic spinal lesions that caused neurologic deterioration and were confirmed on imaging. Affected animals were then euthanized, tumor tissue was excised, and tumor cells were harvested through a process of tissue digestion, cell filtration, centrifugation, and incubation. The selected cell sub-line (RBC-3) was observed to have a growth pattern consistent with that of the parent line, and following intracardiac injection into a host animal, resulted in a statistically significant increase in tumor burden in comparison to the parent MDA-MB-231 breast cancer cells.<sup>27</sup> Similar findings were observed in a mouse model of human breast cancer metastasis, whereby the selected cell sub-line (B02) injected into the tail vein demonstrated a propensity to form rapidly growing osteolytic hindlimb bone metastases.<sup>5</sup> These cancer cell lines may potentially be investigated *in vitro* to identify molecular events important in cellular proliferation, survival, paracrine, and autocrine factors involved in angiogenesis and bone breakdown as well as response to treatment.

### **Analysis of Animal Cancer Metastasis Models**

Real-time imaging is useful for the detection, quantification, staging, and longitudinal monitoring of established tumors and response to treatment in *in vivo* cancer models.<sup>10,27</sup> However, accurate delineation of tumor shape, size, and relationship to surrounding tissues remains a challenge due to the relatively small size of the subject matter. Plain radiographs are cheap, easy to use, and readily available, but can only detect large osteolytic lesions within bone.<sup>16</sup> Nuclear medicine bone scans are sensitive for detecting osteoblastic bone metastases, but may miss small lesions less than one centimeter in diameter and lack specificity due to tracer accumulation in any area of increased bone turnover.<sup>33</sup> Optical imaging is a popular imaging modality currently used in *in vivo* cancer models and is based on the detection of photon emissions from within living tissues. Prior to inoculation, cancer cells are transfected with genes encoding fluorescent or bioluminescent reporter proteins; however, these differ in generating light emitting photons. Fluorescent sources emit light at a particular wavelength in response to an external excitation light source, whereas bioluminescent sources produce light as a

result of a chemical reaction between a systemically distributed substrate, such as injection of luciferin, and the enzyme activity of a reporter protein encoded into cancer cells, such as the Firefly luciferase protein.<sup>10,34</sup> In a mouse model of breast cancer skeletal metastases following intracardiac injection of luciferase transfected MDA-231-B cells, bioluminescence imaging detected bone metastases of approximately 0.5 mm<sup>3</sup> in volume.<sup>22</sup> Real-time identification of tumors at their early stages of growth potentially enables monitoring of disease progression and investigation of efficacy of therapeutic interventions.

Computed tomography (CT) and MRI provide a higher degree of spatial resolution and anatomical definition compared with plain radiographs and are the gold standard for anatomical imaging of bone and soft tissue cancers in human patients. Micro-CT provides quantitative analysis of bone volume, density, and surface area, and has been utilized *in vivo* for longitudinal analysis of tumors in animal models of skeletal metastases and to monitor the effects of potential therapies.<sup>4,29,31</sup> Live animal micro-CT was capable of performing reproducible quantitative analyses of bone volume in an anti-resorptive drug treatment mouse model of breast cancer metastasis to bone.<sup>31</sup> Dedicated small animal MRI scanners use higher strength magnetic-field gradients and higher-sensitivity radiofrequency coils in order to approach the sensitivity and resolution required for imaging small animals.<sup>33</sup> In a mouse model of malignant melanoma, the smallest micro metastasis detectable by animal MRI measured 0.3 mm<sup>3</sup>.<sup>6</sup> Further advances in imaging technology may enable the combination of bioluminescence or fluorescence with CT or MRI to create a three-dimensional, quantitative, cancer-specific image. Potential advantages and disadvantages of the current imaging modalities used for analysis of animal models of skeletal metastasis are summarized in Table 2.

Histopathologic assessment may be used in analysis of skeletal metastases models to complement the clinical and radiological imaging observations and to better understand the pathogenesis of metastasis by more specifically defining the location and extent of tumor growth, morphologic changes of bone and alterations in gene and protein expression.<sup>12,28–30</sup> Histopathologic correlation can be utilized to confirm similarities between animal and human cell lines with



**Table 2.** Imaging modalities available for analysis of skeletal metastases in animal models.

| Imaging method   | Requirement   | Detection  | Advantage  | Disadvantage   |
|--|---|--|--|--|
| Plain radiographs  | Radiographic exposure appropriate to animal size and tissue density   | Only capable of detecting large lesions (eg. >50% vertebral body involvement) or highly sclerotic lesions                                | Cheap, easy to use, readily available, quick, non-invasive. Useful for showing gross morphologic changes.  | Not sensitive at detecting early or small tumours.   |
| Bioluminescence Imaging  | Cancer cell gene transfection with bioluminescent reporter protein (eg. luciferase). Systemic distribution of substrate for light producing chemical reaction (eg. luciferin)                       | Reported detectable size of micrometastasis approximately 0.5 cubic mm   | Relatively cheap, useful for longitudinal monitoring of tumour growth  | Requires systemic injection of substrate to generate photon emission.<br>Detection rate influenced by depth of tissue.<br>Difficult to quantify multimetastatic disease  |
| Fluorescence imaging   | Cancer cell gene transfection with fluorescent reporter protein (eg. green fluorescence protein). External excitation light source to generate photon emission                                      | Reported detectable size of micrometastases approximately 0.06 mm diameter at a depth of 0.5 mm and 1.8 mm diameter at a depth of 2.2 mm | Relatively cheap, useful for longitudinal monitoring of tumour growth.<br>Does not require addition of substrate for photon emission.<br>Non invasive  | Detection rate influenced by depth of tissue.  |
| Nuclear Medicine scans (eg. bone scan, positive emission topography) | Injection of radioactive isotope/tracer, assessment dependent upon specific isotope (eg. perfusion, bone turnover, cell glucose metabolism)   | May detect signal from established tumours from day 1 post inoculation.  | Bone scan sensitive for osteoblastic bone lesions. PET useful to assess tumour viability and metabolism  | Not as sensitive as bioluminescence imaging  |
| Computed Tomography  | Small animal micro-CT with appropriate radiation dose and resolution producing high-resolution images (typically 100 microns or less), data acquisition typically takes 5 to 30 minutes             | Very high sensitivity & specificity for detection of bone lesions, dependent on resolution of the imaging and duration of the scan       | More sensitive than plain radiographs.<br>Allows accurate bone definition, can quantitate volumes and bone density.<br>Non invasive, enabling repeated imaging. Useful for longitudinal monitoring of tumour growth.<br>Potential for 3-dimensional image reconstruction | Lack specificity due to tracer accumulation in any area of increased bone turnover or metabolism.<br>Less sensitive at detecting osteolytic lesions or tumours which have less bone turnover.<br>Poor anatomical definition when used in isolation<br>Expensive infrastructure.<br>Poorer ability to differentiate soft tissue structures.<br>Relatively high dose radiation.<br>High resolution imaging requires that the animal be anaesthetized during scanning.<br>Image quality generally greatly improved by scanning the animal after sacrifice |
| Magnetic Resonance Imaging   | Small animal MRI scanner with higher strength magnetic field gradients and higher sensitivity radiofrequency coils. Potentially able to assess tumoral angiogenesis via injection of contrast media | Reported detectable size of micrometastasis approximately 0.3 cubic mm   | More sensitive than plain radiographs.<br>Best imaging modality currently available for defining soft tissues.<br>Non invasive, enabling repeated imaging. Useful for longitudinal monitoring of tumour growth.  | Expensive infrastructure.<br>High definition of small animal soft tissues currently lacking  |



regards to cytologic appearance of tumor cells and progression of tumor growth.<sup>9,20,23</sup> Furthermore, the mechanisms by which cancer metastases cause clinical symptoms in the experimental animals may be determined through histologic correlation. Vertebral histologic cross-sections in a rat model of intraosseous spinal metastases showed aggressive infiltration and marked osteolytic activity of the tumor cells invading through the vertebral body and compressing the spinal cord, consistent with the clinically observed progressive neurological dysfunction.<sup>36</sup> In a rabbit model of paraplegia caused by spinal tumors, histologic analysis of spine tumor cross-sections from animals with complete paralysis showed a marked reduction in both grey matter and blood vessels to the spinal cord, suggesting that paraplegia may be caused by both direct compressive and ischemic vascular effects to the spinal cord.<sup>16</sup>

Immunohistochemistry and immunotyping through methods such as enzyme-linked immunosorbent assay (ELISA), flow cytometry and polymerase chain reaction may be used to identify markers that contribute to the metastatic potential of tumor cells.<sup>14,30,35</sup> In the development of a mouse model of renal cell carcinoma bone metastases, ELISA analysis of the selected cell subline with increased bone metastatic potential demonstrated greater production of chemokines and growth factors such as vascular endothelial growth factor (VEGF) involved in tumor progression and osteoclast activation than the parent cell line.<sup>14</sup> Further detailed molecular analysis of tumor sections at the metastatic site will provide improved understanding of the temporospatial pattern and pathological mechanisms behind cancer spread to bone and its subsequent growth and invasion into surrounding soft tissues.

## Clinical Application of Animal Cancer Metastasis Models

Animal models are essential for investigating the important molecular mechanisms involved in the metastatic spread of cancer to bone and the testing of promising novel therapies prior to clinical application in human patients.<sup>10,37</sup> The bone marrow microenvironment, incorporating local tissue and tumor-expressed factors, is known to be important in the initial establishment and proliferation of cancer cells in bone.<sup>10,15</sup> Factors involved in physiological and pathological bone turnover and angiogenesis such

as parathyroid hormone-related protein (PTHrP), receptor activator of NF $\kappa$ B ligand (RANKL), VEGF, tumor necrosis factor- $\alpha$ , transforming growth factor  $\beta$ , prostaglandins, and interleukins, have been shown to be expressed in many primary and secondary cancers and have been extensively investigated in animal models of skeletal metastases.<sup>11,14,15</sup> Lelekakis et al found high expression of PTHrP in both primary tumors and bone lesions in a murine breast carcinoma model.<sup>15</sup> Bone metastases induced by parental MDA-231 human breast cancer cells in a xenograft mouse model were shown to highly express bone resorbing and pro-angiogenic factors such as PTHrP, macrophage colony stimulating factor, and VEGF, highlighting the importance of these factors in the bone metastatic cascade.<sup>22</sup> Consequently, the angiogenesis and osteoclastic bone-degradation pathways are effective targets for current and emerging therapies for skeletal metastases.

An important pro-osteoclastogenic factor required for the development and function of bone-resorbing osteoclasts is RANKL. Blocking RANKL has been shown to inhibit breast and prostate cancer-induced osteoclastogenesis and tumor development, growth and progression in bone.<sup>14</sup> Bisphosphonates have also been shown to potently inhibit osteoclast-mediated bone resorption and can reduce skeletal tumor burden and inhibit the formation of bone metastases in vivo, as well as demonstrating clinical application in the treatment of patients with osteolytic bone metastases.<sup>31,34,38,39</sup> Photodynamic therapy, which causes oxygen toxicity and tumor cell necrosis by light activation of an administered photosensitizer accumulated in tumor tissue, has been shown to inhibit tumor growth in several rat models of human breast cancer vertebral metastases, with additional improvement in the structural integrity of vertebral bone when used in conjunction with bisphosphonates.<sup>38–40</sup>

In a metastatic mouse breast cancer model, Takahashi et al demonstrated that expression of the chemokine CCL2 negatively regulated bone metastasis and that CCL2 may act as a negative upstream regulator of intracellular adhesion molecule-1 expression, which is important for determining the capacity for growth, invasion, and metastasis.<sup>35</sup> Overexpression of the  $\alpha v\beta 3$  integrin, a transmembrane protein that integrates intra- and extra-cellular activities and induces tumor cell migration, proliferation and differentiation



has been observed in several experimental models of bone metastasis.<sup>30,34</sup> Treatment with cilengitide, a small molecule inhibitor of  $\alpha v\beta 3$  and  $\alpha v\beta 5$  integrins, resulted in pronounced anti-resorptive and anti-tumor effects in a rat model of breast cancer bone metastasis.<sup>30</sup> Further development and characterization of animal models of skeletal metastasis are necessary to provide suitable platforms on which to identify and test novel therapies.

## Conclusion

Metastatic spread of cancer to the skeleton has the potential to cause severe morbidity, deterioration in function and mobility, and impaired quality of life. To date, there are many established *in vivo* animal models of skeletal metastasis, varying in host animal, type of cancer investigated, method of tumor inoculation and metastatic potential. Further characterization of these models and development of new, novel animal models focusing on specific cancer types and metastatic sites are essential for better understanding the mechanisms behind why and how particular cancers metastasize to, establish within, and invade bone. Ultimately, the identification of key targets for therapeutic intervention, development of novel therapies, and testing of these agents in clinically relevant animal models may be translated into improved treatment, quality of life, and survival of patients with metastatic cancer.

## Author Contributions

Wrote the first draft of the manuscript: CH, GQ. Contributed to the writing of the manuscript: CH, DC, GQ. Agree with manuscript results and conclusions: CH, DC, GQ. Jointly developed the structure and arguments for the paper: GQ, CH. Made critical revisions and approved final version: CH, DC, GQ. All authors reviewed and approved of the final manuscript.

## Funding

This work was supported by the National Health and Medical Research Council of Australia (Fellowship No. 558418), the Austin Health Medical Research Foundation and the Victorian Orthopaedic Research Trust.

## Competing Interests

Authors disclose no potential conflicts of interest.

## Disclosures and Ethics

As a requirement of publication the authors have provided signed confirmation of their compliance with ethical and legal obligations including but not limited to compliance with ICMJE authorship and competing interests guidelines, that the article is neither under consideration for publication nor published elsewhere, of their compliance with legal and ethical guidelines concerning human and animal research participants (if applicable), and that permission has been obtained for reproduction of any copyrighted material. This article was subject to blind, independent, expert peer review. The reviewers reported no competing interests. Provenance: the authors were invited to submit this paper.

## References

1. Arguello F, Baggs RB, Duerst RE, Johnstone L, McQueen K, Frantz CN. Pathogenesis of vertebral metastasis and epidural spinal cord compression. *Cancer*. 1990;65(1):98–106.
2. Mundy GR. Metastasis to bone: causes, consequences and therapeutic opportunities. *Nat Rev Cancer*. 2002;2(8):584–593.
3. Mundy GR. Mechanisms of bone metastasis. *Cancer*. 1997;8(8 Suppl):1546–1556.
4. Mann KA, Lee J, Arrington SA, Damron TA, Allen MJ. Predicting distal femur bone strength in a murine model of tumor osteolysis. *Clin Orthop Relat Res*. 2008;466(6):1271–1278.
5. Garcia T, Jackson A, Bachelier R, et al. A convenient clinically relevant model of human breast cancer bone metastasis. *Clin Exp Metastasis*. 2008;25(1):33–42.
6. Weber MH, Sharp JC, Latta P, Hassard TH, Orr FW. Early detection and quantification of murine melanoma bone metastases with magnetic resonance imaging. *Skeletal Radiol*. 2007;36(7):659–666.
7. Quan GM, Vital JM, Aurouer N, et al. Surgery improves pain, function and quality of life in patients with spinal metastases: a prospective study on 118 patients. *Eur Spine J*. 2011;20(11):1970–1978.
8. Singh AS, Figg WD. *In vivo* models of prostate cancer metastasis to bone. *J Urol*. 2005;174(3):820–826.
9. Al Nakouzi N, Bawa O, Le Pape A, et al. The IGR-CaP1 xenograft model recapitulates mixed osteolytic/blastic bone lesions observed in metastatic prostate cancer. *Neoplasia*. 2012;14(5):376–387.
10. Rosol TJ, Tannehill-Gregg SH, LeRoy BE, Mandl S, Contag CH. Animal models of bone metastasis. *Cancer*. 2003;97(3 Suppl):S748–757.
11. Cossigny D, Quan G. *In vivo* animal models of spinal metastasis. *Cancer Metastasis Rev*. 2012;31(1):99–108.
12. Tatsui CE, Lang FF, Gumin J, Suki D, Shinojima N, Rhines LD. An orthotopic murine model of human spinal metastasis: histological and functional correlations. *J Neurosurg Spine*. 2009;10(6):501–512.
13. Taghian A, Budach W, Zietman A, et al. Quantitative comparison between the transplantability of human and murine tumors into the subcutaneous tissue of NCr/Sed-nu/nu nude and severe combined immunodeficient mice. *Cancer Res*. 1993;53(20):5012–5017.
14. Strube A, Stepina E, Mumberg D, Scholz A, Hauff P, Käkönen SM. Characterization of a new renal cell carcinoma bone metastasis mouse model. *Clin Exp Metastasis*. 2010;27(5):319–330.
15. Lelekakis M, Moseley JM, Martin TJ, et al. A novel orthotopic model of breast cancer metastasis to bone. *Clin Exp Metastasis*. 1999;17(2):163–170.
16. Takahashi M, Ogawa J, Kinoshita Y, Takakura M, Mochizuki K, Satomi K. Experimental study of paraplegia caused by spinal tumors: an animal model of spinal tumours created by transplantation of VX2 carcinoma. *Spine J*. 2004;4(6):675–680.



17. Amundson E, Pradilla G, Brastianos P, et al. A novel intravertebral tumor model in rabbits. *Neurosurgery*. 2005;57(2):341–346.
18. Van der Linde-Sipman JS, van den Ingh TS. Primary and metastatic carcinomas in the digits of cats. *Vet Q*. 2000;22(3):141–145.
19. Langlais LM, Gibson J, Taylor JA, Caswell JL. Pulmonary adenocarcinoma with metastasis to skeletal muscle in a cat. *Can Vet J*. 2006;47(11):1122–1123.
20. Anidjar M, Scarlata E, Cury F, et al. Refining the orthotopic dog prostate cancer (DPC)-1 model to better bridge the gap between rodents and men. *Prostate*. 2012;72(7):752–761.
21. Arguello F, Baggs RB, Frantz CN. A murine model of experimental metastasis to bone and bone marrow. *Cancer Res*. 1988;48(23):6876–6881.
22. Wetterwald A, van der Pluijm G, Que I, et al. Optical imaging of cancer metastasis to bone marrow: a mouse model of minimal residual disease. *Am J Pathol*. 2002;160(3):1143–1153.
23. Passineau MJ, Siegal GP, Everts M, et al. The natural history of a novel, systemic, disseminated model of syngeneic mouse B-cell lymphoma. *Leuk Lymphoma*. 2005;46(11):1627–1638.
24. Biesalski B, Yilmaz B, Buchholz HG, Bausbacher N, Schreckenberger M, Thews O. An allogenic site-specific rat model of bone metastases for nuclear medicine and experimental oncology. *Nucl Med Biol*. 2012;39(4):502–508.
25. Schubert A, Hawighorst T, Emons G, Gründker C. Agonists and antagonists of GnRH-I and -II reduce metastasis formation by triple-negative human breast cancer cells in vivo. *Breast Cancer Res Treat*. 2011;130(3):783–790.
26. Choi JA, Kang EY, Kim HK, Song IC, Kim YI, Kang HS. Evolution of VX2 carcinoma in rabbit tibia: magnetic resonance imaging with pathologic correlation. *Clin Imaging*. 2008;32(2):128–135.
27. Zadnik P, Sarabia-Estrada R, Groves ML, et al. A novel animal model of human breast cancer metastasis to the spine: a pilot study using intracardiac injection and luciferase-expressing cells. *J Neurosurg: Spine*. 2013;18(3):217–225.
28. Liang H, Ma SY, Mohammad K, Guise TA, Balian G, Shen FH. The reaction of bone to tumour growth from human breast cancer cells in a rat spine single metastasis model. *Spine*. 2011;36(7):497–504.
29. Arrington SA, Schoonmaker JE, Damron TA, Mann KA, Allen MJ. Temporal changes in bone mass and mechanical properties in a murine model of tumour osteolysis. *Bone*. 2006;38(3):359–367.
30. Bäuerle T, Komljenovic D, Merz M, Berger MR, Goodman SL, Semmler W. Cilengitide inhibits progression of experimental breast cancer bone metastases as imaged noninvasively using VCT, MRI and DCE-MRI in a longitudinal in vivo study. *Int J Cancer*. 2011;128(10):2453–2462.
31. Johnson LC, Johnson RW, Munoz SA, et al. Longitudinal live animal microCT allows for quantitative analysis of tumour-induced bone destruction. *Bone*. 2011;48(1):141–151.
32. Schuster J, Zhang J, Longo M. A novel human osteoblast-derived severe combined immunodeficiency mouse model of bone metastasis. *J Neurosurg: Spine*. 2006;4(5):388–391.
33. Gauvain KM, Garbow JR, Song SK, Hirbe AC, Weillbacher K. MRI detection of early bone metastases in B16 mouse melanoma models. *Clin Exp Metastasis*. 2005;22(5):403–411.
34. Kaijzel EL, van der Pluijm G, Löwik CW. Whole body optical imaging in animal models to assess cancer development and progression. *Clin Cancer Res*. 2007;13(12):3490–3497.
35. Takahashi M, Miyazaki H, Furihata M, et al. Chemokine CCL2/MCP-1 negatively regulates metastasis in a highly bone marrow-metastatic mouse breast cancer model. *Clin Exp Metastasis*. 2009;26(7):817–828.
36. Mantha A, Legnani FG, Bagley CA, et al. A novel rat model for the study of intraosseous metastatic spine cancer. *J Neurosurg Spine*. 2005;2(3):303–307.
37. Power CA, Pwint H, Chan J, et al. A novel model of bone-metastatic prostate cancer in immunocompetent mice. *Prostate*. 2009;69(15):1613–1623.
38. Hojjat SP, Won E, Hardist MR, Akens MK, Wise-Milestone LM, Whyne CM. Non-destructive evaluation of the effects of combined bisphosphonate and photodynamic therapy on bone strain in metastatic vertebrae using image registration. *Ann Biomed Eng*. 2011;39(11):2816–2822.
39. Won E, Wise-Milestone LW, Akens MK, et al. Beyond bisphosphonates: photodynamic therapy structurally augments metastatically involved vertebrae and destroys tumor tissue. *Breast Cancer Res Treat*. 2010;124(1):111–119.
40. Akens MK, Hardisty MR, Wilson BC, et al. Defining the therapeutic window of vertebral photodynamic therapy in a murine pre-clinical model of breast cancer metastasis using the photosensitizer BPD-MA (Verteporfin). *Breast Cancer Res Treat*. 2010;119(2):325–333.
41. Cowey S, Szafran A, Kappes J, et al. Breast cancer metastasis to bone: evaluation of bioluminescent imaging and microSPECT/CT for detecting bone metastasis in immunodeficient mice. *Clin Exp Metastasis*. 2007;24(5):389–401.
42. Wang L, Rahman S, Lin CY, et al. A novel murine model of human renal cell carcinoma spinal metastasis. *J Clin Neurosci*. 2012;19(6):881–883.
43. Younes MN, Yigitbasi OG, Park YW, et al. Antivascular therapy of human follicular thyroid cancer experimental bone metastasis by blockade of epidermal growth factor receptor and vascular growth factor receptor phosphorylation. *Cancer Res*. 2005;65(11):4716–4727.
44. Molina CA, Sarabia-Estrada R, Gokaslan ZL, et al. Delayed onset of paralysis and slowed tumour growth following in situ placement of recombinant human bone morphogenic protein 2 within spine tumours in a rat model of metastatic breast cancer. *J Neurosurg Spine*. 2012;16(4):365–372.